Nanocrystalline-Cellulose-Reinforced Poly(vinylidenefluoride-*co*-hexafluoropropylene) Nanocomposite Films as a Separator for Lithium Ion Batteries

Boor Singh Lalia, Yarjan Abdul Samad, Raed Hashaikeh

Materials Science and Engineering Program, Masdar Institute of Science and Technology, P. O. Box 54224, Abu Dhabi, United Arab Emirates

Received 26 August 2011; accepted 10 January 2012
DOI 10.1002/app.36783
Published online in Wiley Online Library (wileyonlinelibrary.com).

ABSTRACT: Nanocrystalline cellulose (NCC) was synthesized by the facile acid hydrolysis of Kim Wipes tissue papers and characterized with atomic force microscopy (AFM) and X-ray diffraction (XRD). AFM images confirmed the nanosize of the cellulose nanocrystals, and XRD data revealed the high crystallinity. NCC-reinforced poly(vinylidene fluoride-*co*-hexafluoropropylene) (PH) nanocomposite films were fabricated via an electrospinning method. Different concentrations of NCC in the PH matrix were studied. The effects of the NCC content on the tensile modulus, the variation of tensile modulus with temperature, and the thermal properties of the fabricated nanocomposite films were investigated. It was found that PH + 2 wt % NCC was the optimum composition of the nanocomposite. The addition of 2 wt % NCC in the PH films led to a 75% improvement in the tensile modulus. Dynamic mechanical analysis of the PH nanocomposite films with 2 wt % NCC exhibited high values of tensile modulus in the 30–150°C temperature range. High concentrations of NCC led to decreases in the tensile modulus and thermal properties of the separator. © 2012 Wiley Periodicals, Inc. J. Appl. Polym. Sci. 000: 000–000, 2012

Key words: films; modulus; nanocomposites; reinforcement; thermal properties

INTRODUCTION

Lithium ion batteries (LIBs) with high energy and power densities are highly desirable because of their use in a wide range of applications, from portable devices to electric vehicles/hybrid electric vehicles. Researchers in academia and industry are engaged in developing new materials for anodes, cathodes, and separators/electrolytes to improve the energy and power densities of LIBs. The separator is an important component of LIBs and plays the major role of isolating the anode and cathode to prevent electrical short circuits. It also helps to transport the Li^+ ions between the electrodes during the charging and discharging of the battery. Typically, the three different kinds of electrolytes used in LIBs are liquid electrolytes, gelled electrolytes, and solid electrolytes. The separators used are different in these three configurations. Microporous polyolefins (polypropylene and polyethylene) are commercially available separators widely used in LIBs with liquid electrolytes and gel electrolytes. However, in solid electrolytes, a complex of polymers consisting of poly(ethylene oxide), poly(propylene oxide), poly(ethylene succinate), poly(ethylene imine), and so on with alkali metal salts play the role of electrolyte and separator at the same time.[1–4] However, solid electrolytes suffer from low ionic conductivity and poor electrode–electrolyte electrical contacts. Gel electrolytes are of particular interest because of their high conductivity, which is comparable to liquid electrolytes, and dimensional stability, which is useful for preventing leakage problems and expensive battery sealing. Different host polymers reported for the preparation of gel electrolytes include poly(methyl methacrylate), polyacrylonitrile, poly(ethylene oxide), poly(ethylene glycol), poly(vinylidene fluoride) (PVdF), and poly(vinylidene fluoride-*co*-hexafluoropropylene) (PH).[5–10] Recently, nonwoven electrospun polymer electrolytes/battery separators have been developed because of their uniqueness and controllable parameters, such as fiber size, thickness, porosity, and permeability.[11–13] PVdF, PH, polyacrylonitrile, and poly(methyl methacrylate) (the most widely used polymer for LIBs) have been electrospun and characterized for their use as separators for LIBs.[14–16] PH is

Correspondence to: R. Hashaikeh (rhashaikeh@masdar.ac.ae).

an extensively studied polymer in the preparation of polymer/gel electrolytes for LIBs because of its ability to retain liquid electrolytes by a capacity which is about five times its weight.

There is a need to develop a separator that can be swollen with a liquid electrolyte to achieve a high ionic conductivity for the fast transportation of ions between the electrodes and to achieve high mechanical stability and good electrode–electrolyte electrical contacts. Cellulose is a member of the polysaccharide family and is a material of interest because of its abundant availability, biodegradability, and low cost.[17] Nanocrystals of cellulose can be extracted by the acid hydrolysis of cellulose.[18–20] Nanocrystalline cellulose (NCC) has advantages over conventional nanoparticles, such as SiO_2, Al_2O_3, and TiO_2, which are used for the modification of the electrical and mechanical properties of polymer electrolytes.[21–23] NCC has a whisker shape with a high aspect ratio. It has a high tensile strength, and the modulus of elasticity of the perfect crystal of native cellulose has been calculated by many authors and is estimated to be 138 GPa.[24] Because of these promising properties of NCC, it could be an ideal candidate for reinforcing the polymer matrix for use as a separator/electrolyte in LIBs. NCC has been reported as a reinforcement for biodegradable polymers to produce nanocomposite materials.[25–28] Cellulose nanocrystals have been also used to reinforce poly(oxyethylene)-based solid polymer electrolytes.[29] However, the use of NCC to reinforce electrospun microporous separators of PH has not been studied before.

In this work, NCC was used to reinforce electrospun PH nanocomposite separators. Different concentrations of NCC were dispersed in 15 wt % solutions of PH in acetone/dimethylacetamide (70 : 30 w/w) to prepare nonwoven electrospun nanocomposite films. Tensile strength, dynamic mechanical analysis (DMA), atomic force microscopy (AFM), and differential scanning calorimetry (DSC)/thermogravimetric analysis (TGA) studies of the electrospun films were conducted to analyze the effects of the NCC dispersion in the PH matrix.

EXPERIMENTAL

Extraction of NCC

KIMTECH Science KimWipes Delicate Task Wipes from Kimberly-Clark Professional were ground and used as sources of cellulose (Kimberly-Clark Inc., Mississauga, Ontario). Sulfuric acid (95–97%, reagent grade) was purchased from Scharlau. Ground cellulose (10 g) was mixed with 91 mL of 64% (w/w) H_2SO_4 with a Varian Dissolution System (VK7010) at 45°C with 250-rpm agitation. After 10 min, 187 mL of 50% H_2SO_4 was added. The mixture was centrifuged once at 23°C for 10 min at 4700 rpm with an Allegra 25R centrifuge. The top layer was decanted, and the bottom layer was centrifuged two more times. The bottom layer was collected and dialyzed for 3 days until the pH was almost neutral. The resulting white suspension was weighed and then sonicated with a Hieschler Ultrasonic Processor UP400S for 2 min. After dialysis, we calculated the yield by withdrawing a known amount of a small sample and obtaining its oven-dried weight. The yield was calculated on the basis of the solid product weight after hydrolysis and drying compared to the starting weight. The white suspension in water was freeze-dried with a VirTis Wizard 2.0 freeze drier to obtain NCC and was used for the preparation of the NCC/PH nanocomposite films.

Electrospinning of the PVdF–fluoropropylene/NCC nanocomposite separator

PH (Kynar Powerflex LBG), acetone (Aldrich), and dimethylacetamide (Aldrich) were used as received. A clear and uniform solution of 15 wt % PH was prepared in a binary mixture of acetone and dimethylacetamide with a weight ratio of 7 : 3 and was stirred with a magnetic stirrer. The different compositions of PH and NCC are written as PH + xNCC (where x = 1, 2, 3, 4, or 5 wt %) and were prepared by the dispersion of different weight percentages of NCC in the PH solution. The PH and PH + xNCC solutions were loaded in a 10-mL glass syringe with a luer lock steel tip connected to a SS needle by a PTFE pipe. A Nanon-01A electrospinning setup (MECC, Japan) was used for electrospinning the polymer solution. A potential difference of 19 kV was generated between the needle and an aluminum grounded target placed 15 cm from the tip of the needle. The electrospun nanocomposite separators of PH with and without NCC were collected on an aluminum drum at 25°C and dried at 50°C for 24 h in a conventional oven. The thickness of the nanocomposite separators was in the range 60–70 μm.

Characterization

NCC was characterized with AFM (Asylum Research, MFP-3D^{TM}Stand Alone) and X-ray diffraction (XRD; PANalytical, Empyrean) analysis. The samples for AFM study were prepared by sonication of a 1 wt % NCC solution in ethanol for 15 min at three intervals to avoid the overheating of the material. The solution (10 μL) was placed on a glass slide and dried at room temperature. AFM was performed with a silicon tip with a radius of 10 nm, a resonance frequency of about 70 kHz, and a spring constant of 2 N/m in the noncontact tapping mode.

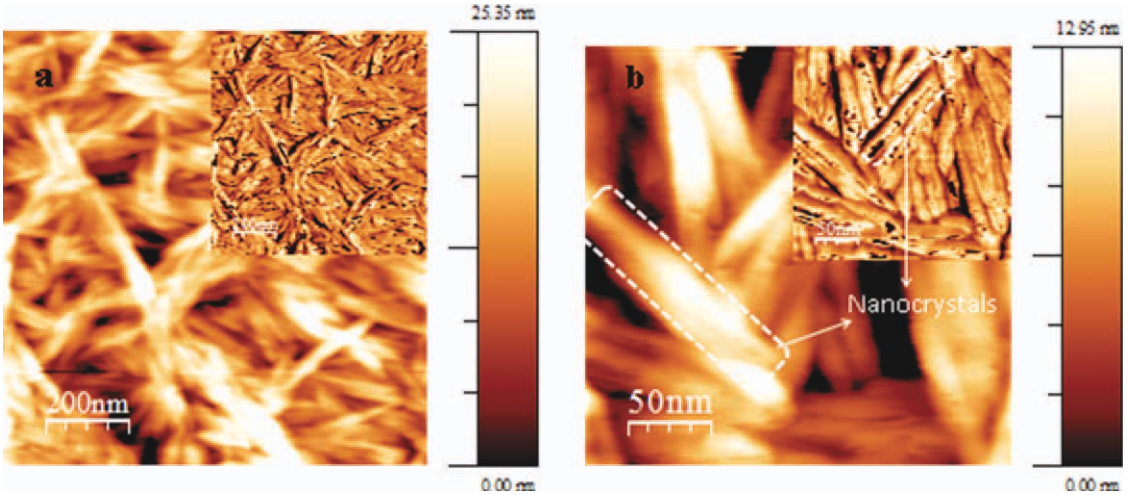

Figure 1 AFM micrographs of NCC at (a) 2-μm and (b) 500-nm resolutions. [Color figure can be viewed in the online issue, which is available at wileyonlinelibrary.com.]

The morphology of the electrospun separator was examined by scanning electron microscopy (SEM; FEI Quanta FEG 250). The Young's modulus and tensile strength values of the PH and PH + *x*NCC electrospun nanocomposite separators were measured by an Instron model 5982 instrument equipped with a load cell of 5 kN at a strain rate of 2 mm/min. The dog-bone shaped specimens, having lengths of 65 mm, were cut from the separator films at thicknesses of about 60–70 μm. Three samples for each composition were tested to ensure the reproducibility of the test results. A small variation of 5–10% in the stress–strain values was observed; this may have been due to the minute thicknesses of the samples and the handling of such samples while they were loaded in the test cells. DMA (PerkinElmer DMA 8000) was used to investigate the variation of Young's modulus in the 30–150°C temperature range in tension deformation mode at a frequency of 1 Hz and a heating rate of 2°C/min on rectangular samples with dimensions of 5 × 30 mm^2. The thermal stability of the electrospun films was characterized by DSC (PerkinElmer DSC 4000) and TGA (PerkinElmer TGA 4000). DSC was performed at a heating rate of 10°C/min over a temperature range of 30–400°C in a nitrogen atmosphere. TGA of the nanocomposite separator was studied in the 25–800°C temperature range in a nitrogen atmosphere with a scan rate of 10°C/min.

RESULTS AND DISCUSSION

The hydrolysis of the ground cellulose powder was carried out in 64% H_2SO_4 by modification of the reported hydrolysis process to extract NCC.[19] The amorphous part of the cellulose was digested rapidly by the acid, whereas crystalline cellulose was retained in the solution under the employed

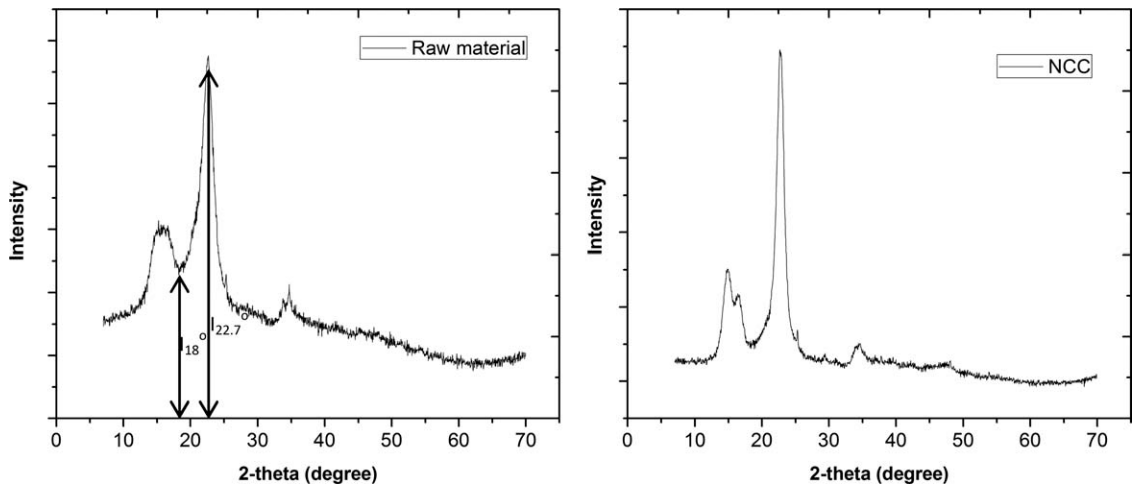

Figure 2 XRD diffractograms of the (a) raw material (Kim wipes) and (b) NCC.

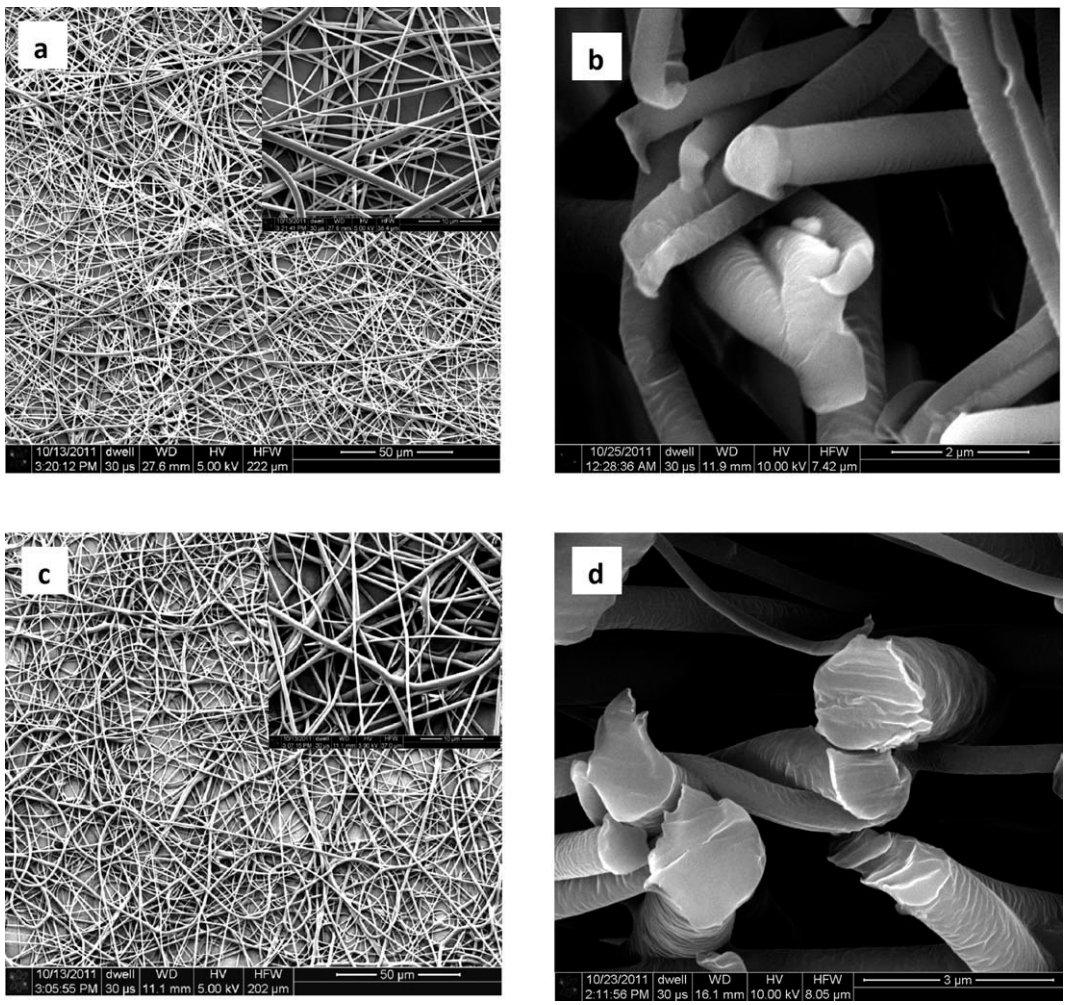

Figure 3 SEM images of the (a) surface and (b) cross section of PH and (c) surface and (d) cross section of the PH + 2NCC electrospun separators.

conditions, that is, 64% H_2SO_4 at 45°C for 10 min.[20] NCC was separated from the amorphous part and acid was removed by subsequent centrifugation followed by dialysis and then freeze drying. The formation of NCC was confirmed by topographical microimages from the AFM and XRD studies. The surface topography of NCC with AFM imaging is shown in Figure 1. The inset shows the phase retrace of the surface topography of the nanocrystals. The two-dimensional images revealed the rodlike nanocrystals of NCC, and the average diameter of the crystals was estimated from the roughness of the surface. NCC had an average diameter of about 20 nm and a length of about 200 nm. XRD diffractograms of the raw material (KimWipes) and NCC are shown in Figure 2(a,b), respectively. The characteristic peaks of cellulose I were found at $2\theta = 14.7$, 16.4, and 22.6°.[30] NCC had intense and sharp peaks arising from the nanocrystals of cellulose. The crystallinities of the NCC and raw material were calculated with the Segel method:[31]

$$\text{Crystallinity}\,(\%) = \frac{I_{22.7^\circ} - I_{18^\circ}}{I_{22.7^\circ}} \times 100 \qquad (1)$$

where $I_{22.7^\circ}$ is the intensity of the peak at 22.7° (2θ) and corresponds to crystalline and amorphous cellulose, respectively, and I_{18° is the intensity of the peak due to amorphous cellulose only. The percentage crystallinity of NCC and the raw material were found to be 87 and 70%, respectively. However, NCC had traces of amorphous cellulose; this occurred during the separation of the bottom layer of the NCC (as discussed in the Experimental section) from the top layer, which contained amorphous cellulose.

Figure 3 shows SEM images of the nanofibers of PH and PH + 2NCC prepared from a solution of 70 wt % acetone and 30 wt % dimethylacetamide with the electrospinning method. Acetone was used as a solvent because of its low boiling point (56°C), and dimethylacetamide was used as a nonsolvent (a high boiling point, 166°C, solvent). The porosity and

thickness of electrospun separators can be altered by the variation of the viscosity of the solution, the speed of the spinneret, the flow rate of the solution, and so on. However, in this study, all of the parameters were kept constant to study the effect of the NCC dispersion in PH on the mechanical properties of the separator. The fibers obtained with electrospinning were different in diameter and were found to be in the range of 200 nm to 1 μm. The solution viscosity is an important parameter in determining the fiber diameter and morphology of the electrospun fibers, and an optimum concentration of solution is required to obtain nonwoven membranes with a smooth and continuous fibrous structure.[32] The addition of NCC increases the viscosity of the PH solution, which affects the average diameter of the fibers. Figure 3(b) shows the SEM images of the PH+ 2NCC fibers; the addition of NCC increases the average diameter of the fibers. The size distribution of the nanofibers is shown well by the surface SEM images of the fiber mat film. However, the morphology could not be revealed because of charge accumulation, even after the sputtering of a few nanometers of conducting metal film on the nonconducting fiber mat. We, therefore, took SEM images of the cross section to see the morphology of the individual fibers. There was low charge accumulation in the cross-sectional imaging of the fiber mat because of its highly porous structure in the cross section. Also, because of the vertical orientation of the sample charge accumulation was minimized, and thus, a clear image with a higher resolution was obtained; this revealed the surface morphology of the individual fibers. SEM images of the cross sections of the PH and PH + 2NCC fibers are shown in Figure 3(c,d), respectively. The cross-sectional SEM images indicated that the morphology of the base polymer PH was not altered with the addition of NCC. Also, the addition of NCC in the PH matrix did not lead to the formation of cracks, and the shortening of fibers in the electrospun separator indicated that NCC was physically entrapped inside the nanocomposite fibers.

NCC was dispersed inside the polymer matrix to improve the mechanical properties of the composite material. Generally, polymers consist of entangled molecular chains in the solid state, and when dissolved in a solvent, they swell, and their volume increases. NCC was dispersed in the swollen PH and electrospun to obtain a nonwoven polymer separator. After the evaporation of the solvent from the polymer fibers, NCC reinforced the nonwoven polymer films. This led to a more rigid structure and a decrease in the polymer stretching. This hypothesis was consistent with the tensile studies discussed in the next paragraph.

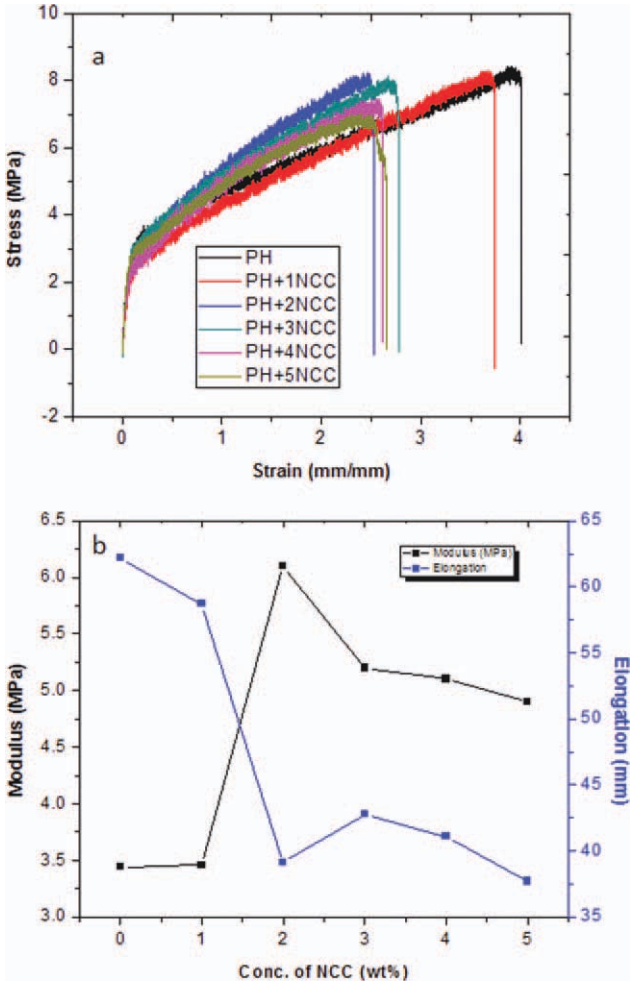

Figure 4 (a) Stress–strain profiles of PH and PH + *x*NCC and (b) variation of Young's modulus and elongation with the concentration of NCC in the PH matrix. [Color figure can be viewed in the online issue, which is available at wileyonlinelibrary.com.]

The tensile strength and tensile modulus are important properties of a separator, and high values are desirable because of the stress encountered during the preparation process (i.e., winding and stacking) of the battery. The stress–strain behavior of PH and PH + *x*NCC is shown in Figure 4(a). The separator without NCC had a high strain at its break point and started decreasing with the addition of NCC. We observed that the addition of NCC did not affect the tensile strength of the nanocomposite separator up to a composition of 3 wt % NCC. However, the tensile strength started decreasing at high concentrations of NCC above 3 wt %. The tensile modulus and elongation were calculated from the stress–strain curves and are shown in Figure 4(b). The addition of 2 wt % NCC significantly improved the tensile modulus of the electrospun nanocomposite separator from 3.4 to 6.1 MPa without deteriorating its tensile strength. In contrast, simultaneously, the

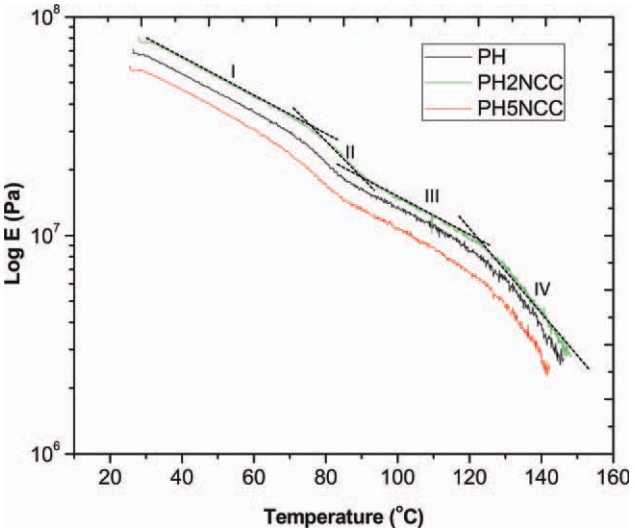

Figure 5 Storage modulus (E) variation with temperature of (a) PH, (b) PH + 2NCC, and (c) PH + 5NCC in the 30–150°C temperature range. [Color figure can be viewed in the online issue, which is available at wileyonlinelibrary.com.]

elongation length decreased. In previously reported results, cellulose whiskers were used to reinforce solution-cast and *in situ* polymerized separators for LIBs with enhanced mechanical properties.[33–36] However, the results could not be compared quantitatively because of the different fabrication techniques. In general, electrospun fibers are highly porous, with very small diameters and different orientations. This results in a lower mechanical strength compared to solution cast polymer separators. The increase in the tensile modulus of the nanocomposite separator was attributed to the stiff nature of the NCC nanocrystals dispersed inside the PH nanofibers. Hence, the addition of NCC led to an increase in the stiffness of PH and decreases in its elongation and in the value of the strain at break. PH + 2NCC was the optimum composition of the nanocomposite separator, with an enhanced mechanical strength. For high concentrations of NCC above 2 wt %, there seemed to be an agglomeration of NCC inside the matrix; this resulted in an NCC/NCC interaction taking over the effect of the NCC/PH interaction and resulting in an earlier failure and a further decrease in the elongation and tensile modulus. At higher concentrations of NCC inside the PH matrix, the agglomerates of NCC increased the microstructural/nanostructural inhomogeneity of the material and acted as sites of stress concentration; this decreased the strength and the tensile modulus of the nanocomposite.

Furthermore, the variation of the tensile modulus with temperature was studied via DMA in the tensile mode, and the results are shown in Figure 5. PH + 2NCC had a high tensile modulus in the 30–150°C temperature range. The tensile modulus decreased gradually with increasing temperature, regions I and III, because of the heating effect. A change in the modulus behavior was observed in the 80–100°C temperature range (region II). This was due to the melting of the short polymer side chains of the host polymer,[7] and these results were consistent with the DSC results discussed in the next paragraph. A sharp decrease in the modulus was observed above 120°C (region IV), and this was due to the softening of PH near its melting point (135°C). The DMA results revealed that the PH + 2NCC nanocomposite separator had a higher tensile modulus than pure PH and a good thermomechanical stability.

The thermal properties of the nanocomposite separators were investigated by TGA, and the thermograms are given in Figure 6(a). For the base polymer PH, the onset decomposition temperature was

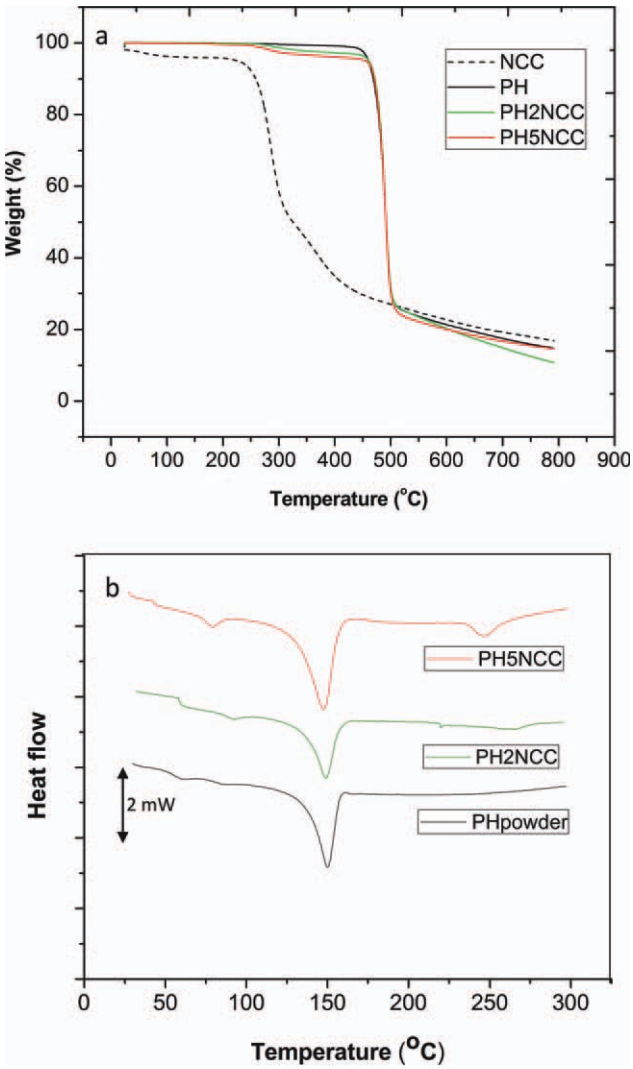

Figure 6 (a) TGA and (b) DSC thermograms of the PH and PH + *x*NCC films. [Color figure can be viewed in the online issue, which is available at wileyonlinelibrary.com.]

450°C, and the onset decomposition temperature for NCC was 255°C. The decomposition temperature of PH was not affected by the dispersion of NCC; however, the addition of NCC increased the weight loss in the 300–450°C temperature range. This observation indicated that there was no chemical interaction between NCC and the PH matrix, and NCC was compatible with the PH polymer. Figure 6(b) shows the thermograms of PH powder and PH with 2 and 5 wt % NCC. Two endothermic peaks were observed at 50 and 150°C; the first peak was due to the melting of the side chains of the polymer, and the second endothermic peak was due to the melting of PH. The addition of NCC in PH did not affect the melting temperature of the polymer matrix and, thus, confirmed the physical interaction between NCC and PH. However, a new endothermic peak appeared at 250°C for PH + 5NCC. This peak was due to the decomposition of NCC.

These studies indicated that the produced nanocomposite separator had excellent thermal and mechanical properties suitable for its application in LIBs. The electrochemical study of the nanocomposite separator is underway to validate its performance in LIBs.

CONCLUSIONS

NCC was synthesized by a facile chemical route and was dispersed in a PH matrix to improve its mechanical strength. Tensile and DMA studies revealed that the addition of 2 wt % NCC in PH improved it mechanical strength in the 30–150°C temperature range. Thermal analysis with DSC/TGA indicated that addition of NCC did not deteriorate the thermal properties of the PH nanocomposite separator. The data also confirmed the physical interaction between NCC and the electrospun PH fibers. PH with 2 wt % NCC had optimum mechanical and thermomechanical properties suitable for its use as a separator in LIBs.

References

1. Wright, P. V. British Polym J 1975, 7, 319.
2. Watanabe, M.; Rikukawa, M.; Sanui, K.; Ogata, N.; Kato, H.; Kobayashi, T.; Ohtaki, Z. Macromolecules 1984, 17, 2902.
3. Watanabe, M.; Oohashi, S.; Sanui, K.; Ogata, N.; Kobayashi, T.; Ohataki, Z. Macromolecules 1985, 18, 1945.
4. Harris, C. S.; Shriver, D. F.; Ratner, M. A. Macromolecules 1986, 19, 987.
5. Kakuda, S.; Momma, T.; Osaka, T.; Apetecchi, G. B.; Scrosati, B. J Electrochem Soc 1995, 142, L1.
6. Tsuchida, E.; Ohno, H.; Tsunemi, E. Electrochim Acta 1983, 28, 591.
7. Jiang, Z.; Caroll, B.; Abraham, K. M. Electrochim Acta 1997, 42, 2667.
8. Fuller, J.; Breda, A. C.; Carlin, R. T. J Electrochem Soc 1997, 144, L67.
9. Singh, H. P.; Sekhon, S. S. Eur Polym J 2003, 39, 93.
10. Yoshimoto, N.; Niida, Y.; Egashira, M.; Morita, M. J Power Sources 2006, 163, 238.
11. Li, X.; Cheruvally, G.; Kim, J. K.; Choi, J. W.; Ahn, J. H.; Kim, K. W.; Ahn, H. J. J Power Sources 2007, 167, 491.
12. Cho, T. H.; Tanaka, M. Onishi, H.; Kondo, Y.; Nakamura, T.; Yamazaki, H.; Tanase, S.; Sakai, T. J Power Sources 2008, 181, 155.
13. Carol, P.; Ramakrishnan, P.; John, B.; Cheruvally, G. J Power Sorces 2011, 196, 10156.
14. Kim, J. K.; Manuel, J.; Chauhan, G. S.; Ahn, J. H.; Ryu, H. S. Electrochim Acta 2010, 55, 1366.
15. Liu, F.; Hashim, N. A.; Liu, Y.; Moghareh Abed, M. R.; Li, K. J Membr Sci 2011, 375, 1.
16. Dong, Z.; Kennedy, S. J.; Wu, Y. J Power Sources 2011, 196, 4886.
17. French, A. D. Carbohydr Res 1978, 61, 67.
18. Bai, W.; Holbery, J.; Li, K. Cellulose 2009, 16, 455.
19. Lu, P.; Hsieh, Y. L. Carbohydr Polym 2010, 82, 329.
20. Hashaikeh, R.; Hu, T. Q.; Berry, R. U.S. Pat. Appl. 20100286387 (2010).
21. Kim, J. W.; Ji, K. S.; Lee, J. P.; Park, J. W. J Power Sources 2003, 119–121, 415.
22. Nookala, M.; Kumar, B.; Rodrigues, S. J Power Sources 2002, 111, 165.
23. Liu, Y.; Lee, J. Y.; Hong, L. J Appl Polym Sci 2003, 89, 2815.
24. Zimmermann, T.; Pöhler, E.; Geiger, T. Adv Eng Mater 2004, 6, 754.
25. Favier, V.; Cavaille, J. Y.; Canova, G. R.; Shrivastava, S. C. Polym Eng Sci 1997, 37, 1732.
26. Azizi Samir, M. A. S.; Alloin, F.; Dufresne, A. Biomacromolecules 2005, 6, 612.
27. Petersson, L.; Kvien, I.; Oksman, K. Compos Sci Technol 2007, 67, 2535.
28. Krishnamachari, P.; Hashaikeh, R.; Tiner, M. Micron 2001, 42, 751.
29. Azizi Samie, M. A. S.; Alloin, F.; Gorecki, W.; Sanchez, J. Y.; Dufresne, A. J Phys Chem B 2004, 108, 10845.
30. Wada, M.; Haux, L.; Sugiyama, J. Biomacromolecules 2004, 5, 1385.
31. Segel, L.; Creely, J. J.; Martin, A. E.; Conard, C. M. Text Res J 1959, 29, 786.
32. Gupta, P.; Elkins, C.; Long, T. E.; Wilkes, G. L. Polymer 2005, 46, 4799.
33. Samira, M. A.; Alloin, F.; Sanchez, J. Y.; Dufresne, A. Polymer 2004, 45, 4149.
34. Ren, Z.; Liu, Y.; Sun, K.; Zhou, X.; Zhang, N. Electrochim Acta 2009, 54, 1888.
35. Alloin, F.; Aprea, A. D.; El Kissi, N.; Dufresne, A.; Bossard, F. Electrochim Acta 2010, 55, 5186.
36. Chiappone, A.; Nair, J. R.; Gerbaldi, C.; Jabbour, L.; Bongiovanni, R.; Zeno, E. J Power Sources 2011, 196, 10280.